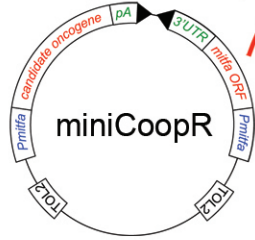
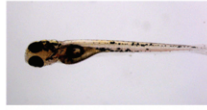


Inject miniCoopR plasmid into single-cell embryos

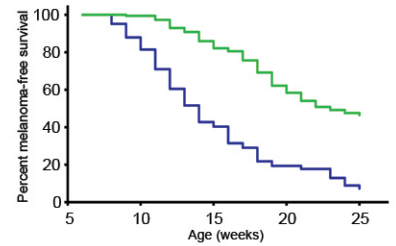


Tg(mitfa:BRAF^{V600E}); p53(lf); mitfa(lf)

Select transgenic embryos with rescued melanocytes

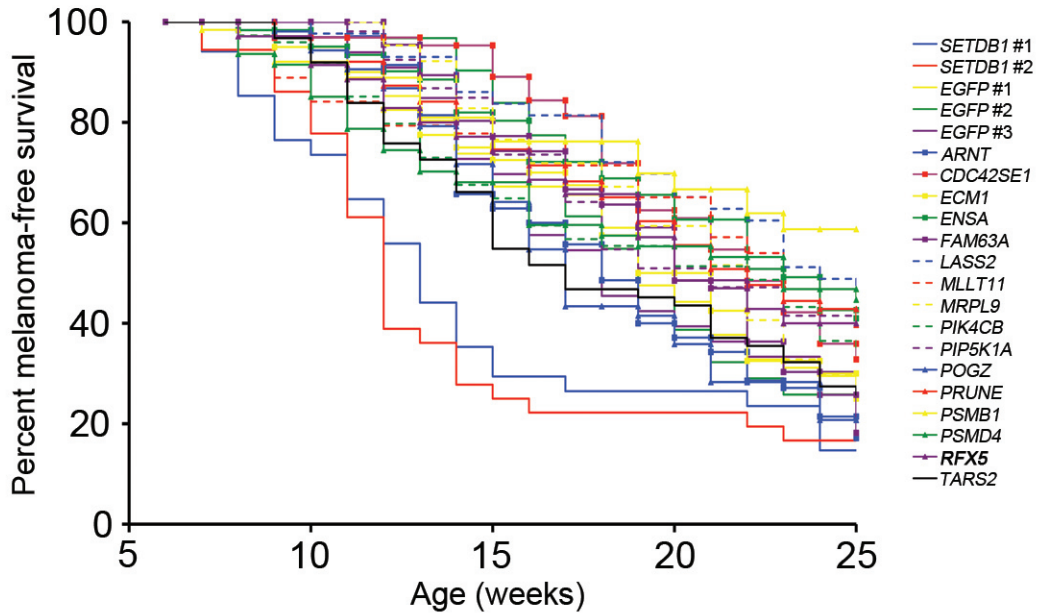


Score for morphologic appearance of tumors and determine tumor incidence



Supplementary Figure 1 | Strategy for assessing candidate melanoma genes

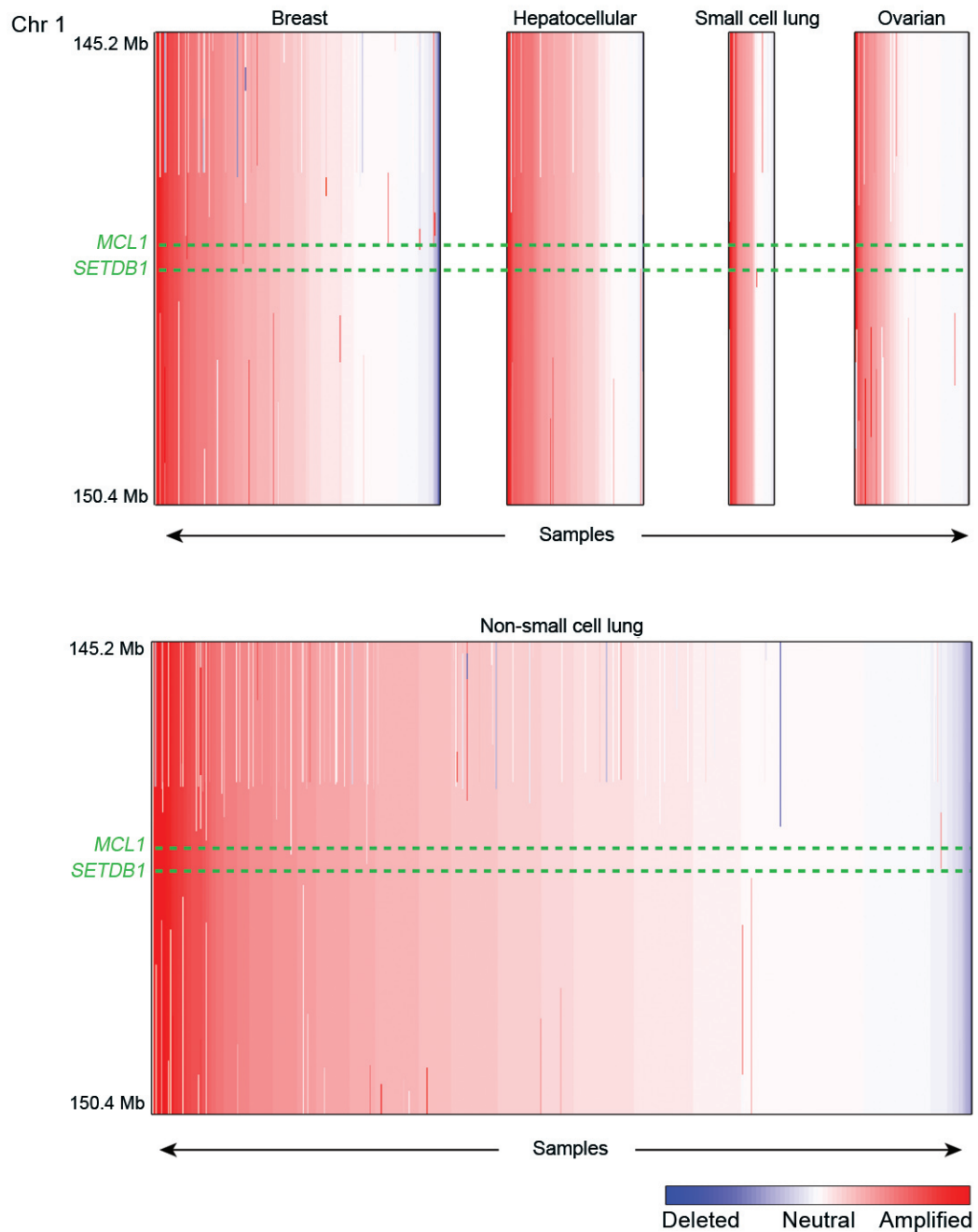
Candidate genes that are both recurrently amplified and overexpressed in human melanomas were cloned into the miniCoopR vector. Injection of a miniCoopR plasmid results in rescue of animals bearing a *mitfa(lf)* mutation. Since *Mitfa* rescues cell-autonomously¹, rescued melanocytes contain the miniCoopR plasmid and its candidate gene cargo. Animals with rescued melanocytes were selected then monitored for tumor onset. *Pmitfa*, a 2.1 kb fragment of the zebrafish *mitfa* gene promoter; *TOL2*, *Tol2* transposon arms that mediate transposase-directed integration; and *pA*, polyadenylation signal.



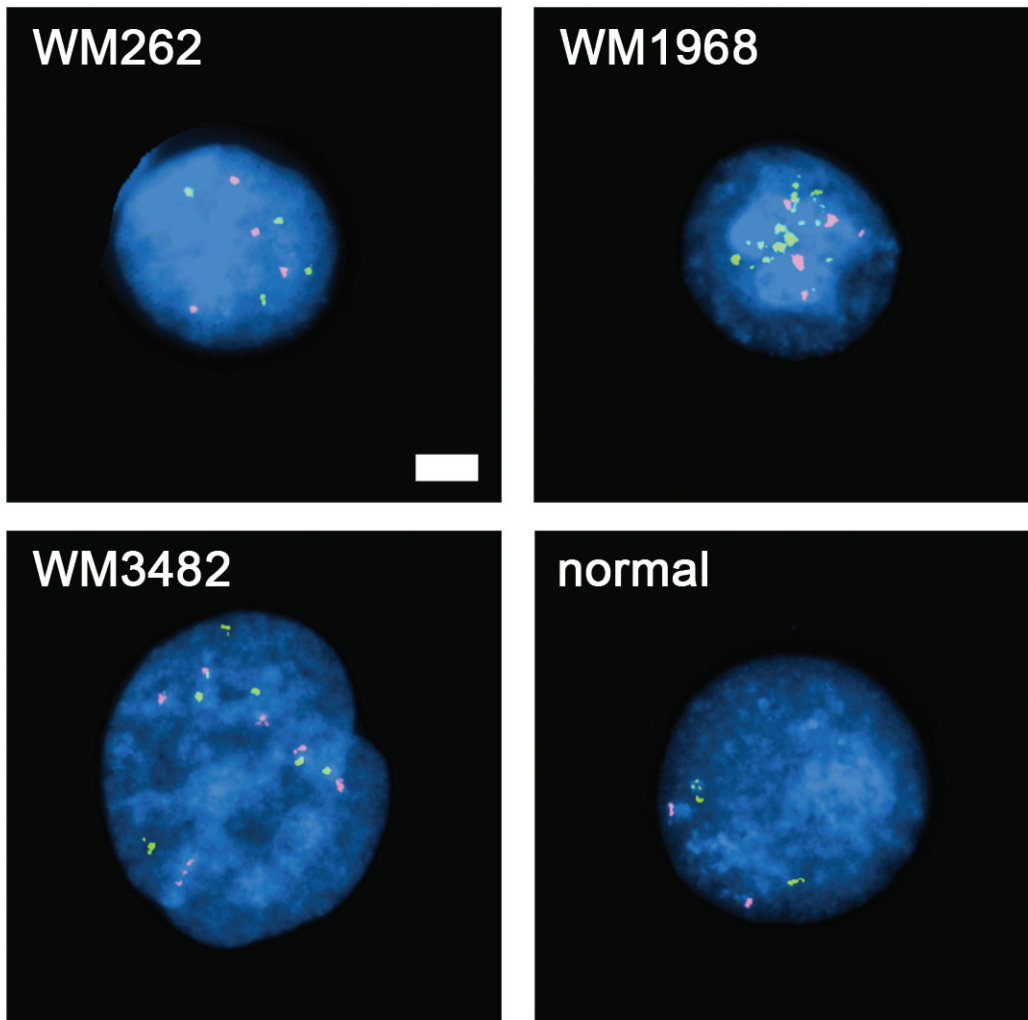
Candidate oncogene	Median tumor onset (wks)	No. animals	p value
<i>SETDB1</i> trial 1	13	34	1.7×10^{-4}
<i>SETDB1</i> trial 2	12	36	1.4×10^{-5}
<i>SETDB1</i> average	12	70	9.4×10^{-7}
<i>EGFP</i> trial 1	19	61	n/a
<i>EGFP</i> trial 2	19	31	n/a
<i>EGFP</i> trial 3	18	33	n/a
<i>EGFP</i> average	19	125	n/a
<i>ARNT</i>	18	70	0.09
<i>CDC42SE1</i>	22	64	0.04
<i>ECM1</i>	21	40	0.86
<i>ENSA</i>	23	61	0.05
<i>FAM63A</i>	20	66	0.65
<i>LASS2</i>	24	43	0.03
<i>MLLT11</i>	23	63	0.07
<i>MRPL9</i>	22	64	0.49
<i>PIK4CB</i>	22	74	0.74
<i>PIP5K1A</i>	21	53	0.31
<i>POGZ</i>	17	53	0.12
<i>PRUNE</i>	22	63	0.17
<i>PSMB1</i>	>25	63	2.9×10^{-4}
<i>PSMD4</i>	23	47	0.30
<i>RFX5</i>	20	35	0.40
<i>TARS2</i>	17	62	0.25

Supplementary Figure 2 | Melanoma-free survival curves and median tumor incidence values for 1q21 candidate genes

p-values were derived from logrank χ^2 values.

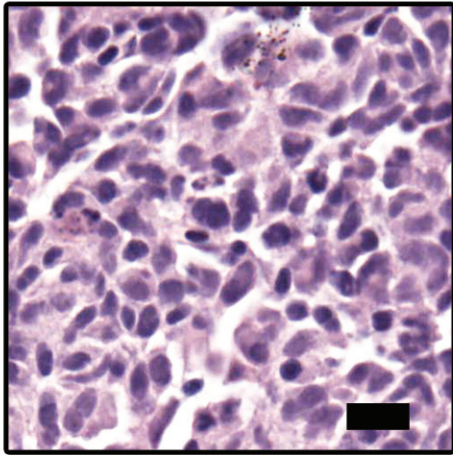


Supplementary Figure 3 | Copy number profiles of the 1q21 interval in different cancer tissues
 Tumor type is shown across the top and genomic location on the left. The positions of *SETDB1* and *MCL1* are indicated (dashed lines).

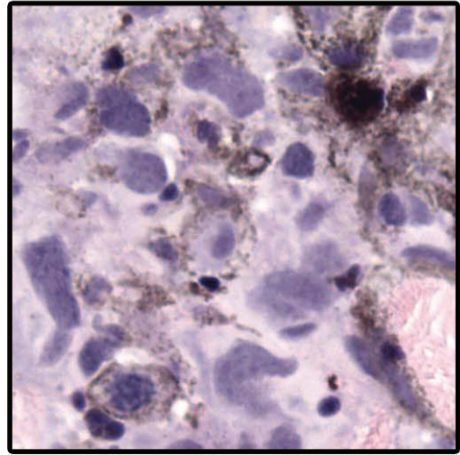


Supplementary Figure 4 | Fluorescence in situ hybridization to the *SETDB1* locus demonstrates amplification in melanoma short-term cultures

FISH analysis of melanoma samples using green and red-labeled BAC probes to detect the *SETDB1* locus and the centromere of chromosome 1, respectively. Interphase nuclei are shown for WM262, WM1968 and WM3482 melanoma short-term cultures, and for normal lymphocytes. These data are consistent with focal (WM1968) and broader amplifications (WM262 and WM3482) at the *SETDB1* locus.



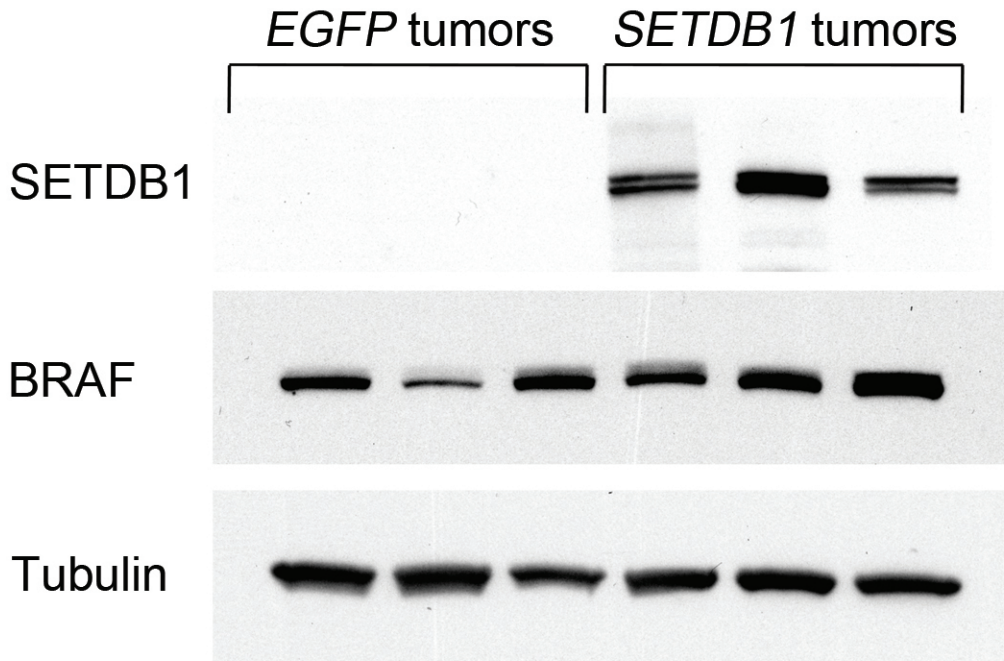
miniCoopR-*EGFP*



miniCoopR-*SETDB1*

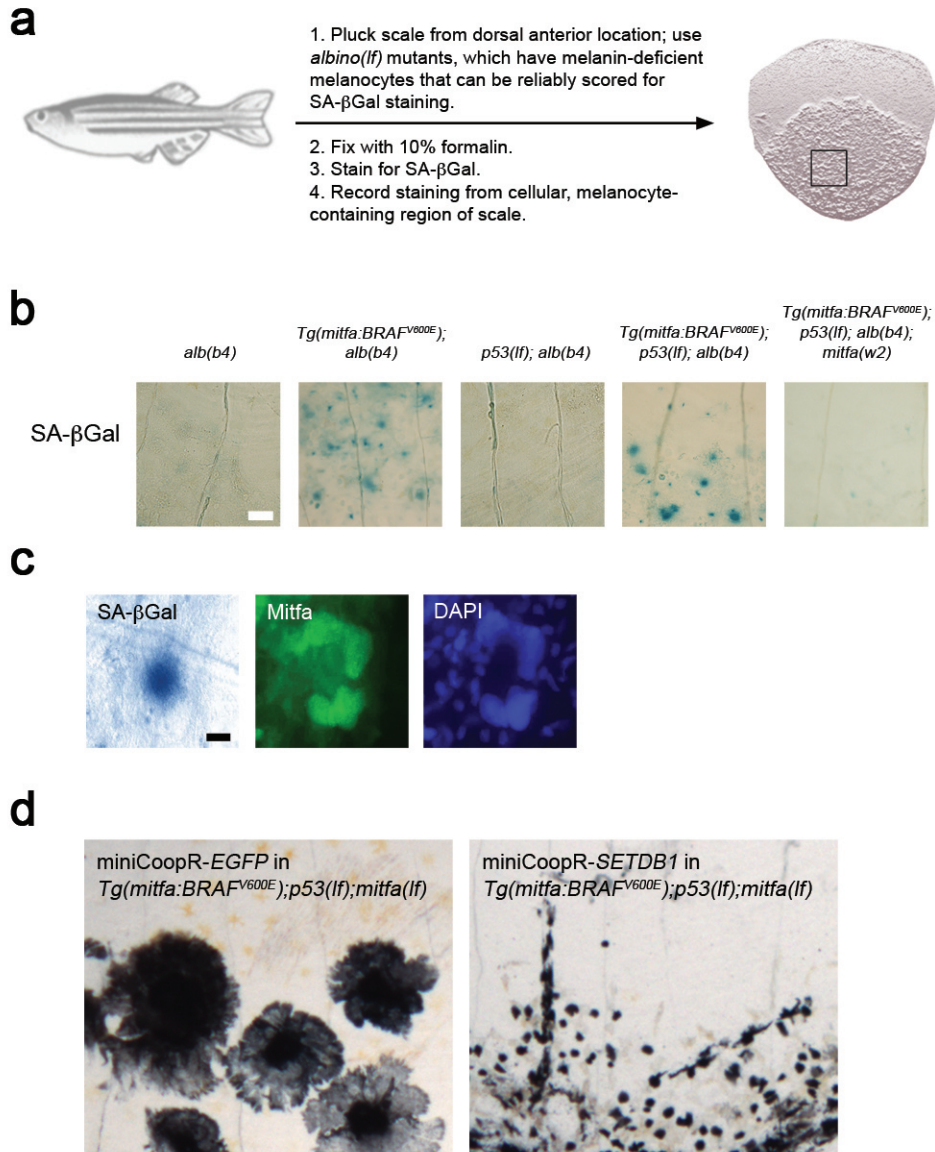
Supplementary Figure 5 | miniCoopR-*SETDB1* melanomas display extensive nuclear pleomorphism and larger nuclei

Melanomas expressing *SETDB1* have greater nuclear pleomorphism and, for most nuclei, a larger nuclear size than control *EGFP*-expressing melanomas. Scale bar = 10 μ m.



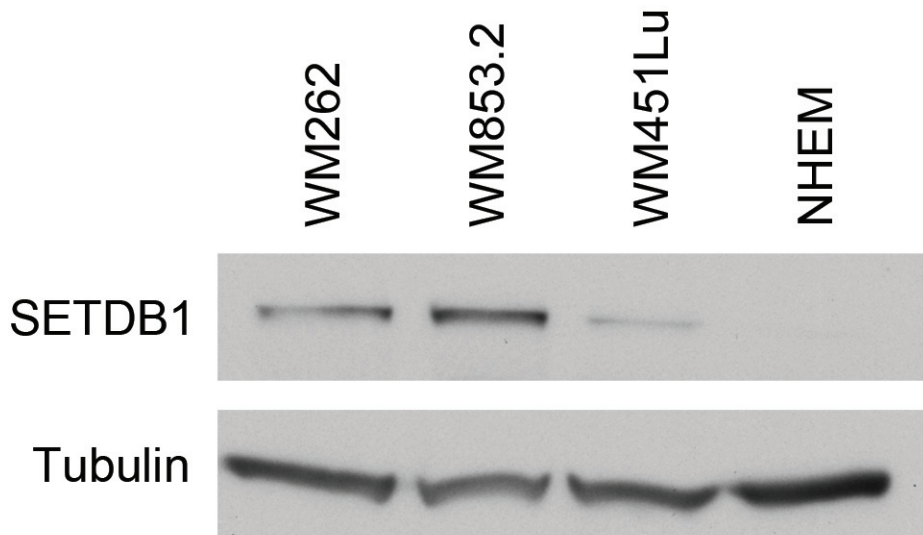
Supplementary Figure 6 | BRAF(V600E) protein levels are similar in miniCoopR-EGFP and miniCoopR-SETDB1 melanomas

Western blot of protein lysates from miniCoopR-EGFP (left) and miniCoopR-SETDB1 (right) melanomas. Zebrafish melanomas from MiniCoopR-SETDB1 injected animals express a protein doublet of approximately 150kDa recognized by anti-SETDB1 antisera.



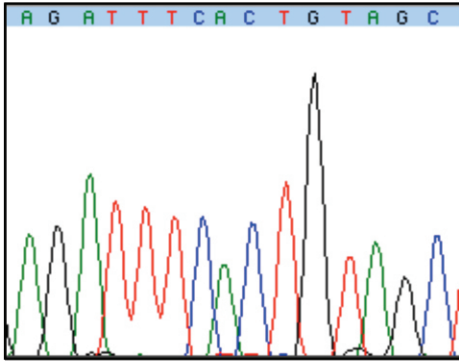
Supplementary Figure 7 | *BRAF^{V600E}* induces senescence of zebrafish scale-associated melanocytes

a, Procedure for performing senescence-associated β -galactosidase (SA- β Gal) staining of scale melanocytes. All assays were performed in an *albino(lf)* background so that melanin pigment did not interfere with the β Gal signal. **b**, SA- β Gal staining of scales. SA- β Gal-positive cells are absent in a *mitfa(lf)* background (right), indicating the cells are melanocytes. Scale bar = 50 μ m. **c**, Mitfa staining confirms that SA- β Gal-positive cells are melanocytes. Scale bar = 10 μ m. **d**, Morphological differences between *EGFP* (left) and *SETDB1* (right) expressing melanocytes.



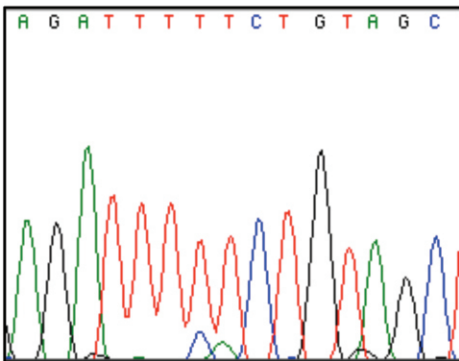
Supplementary Figure 8 | SETDB1 expression levels in melanoma short-term cultures used in this study

Western blot of protein lysates from WM262 (high), WM853.2 (high), and WM451Lu (low) in comparison with normal human embryonic melanocytes (NHEM).



WM1968 *BRAF* wild type

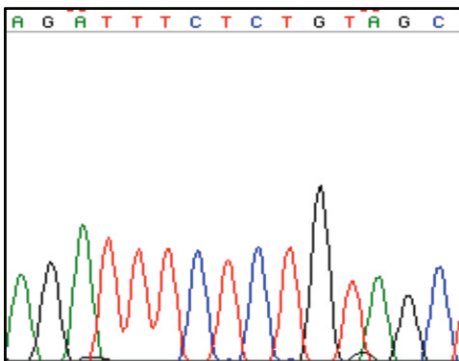
600
 GCT ACA GTG AAA TCT
 CGA TGT CAC TTT AGA
A T V K S



WM262 *BRAF(V600E)* heterozygous

600
 GCT ACA GAA AAA TCT
 CGA TGT CTT TTT AGA
A T E K S

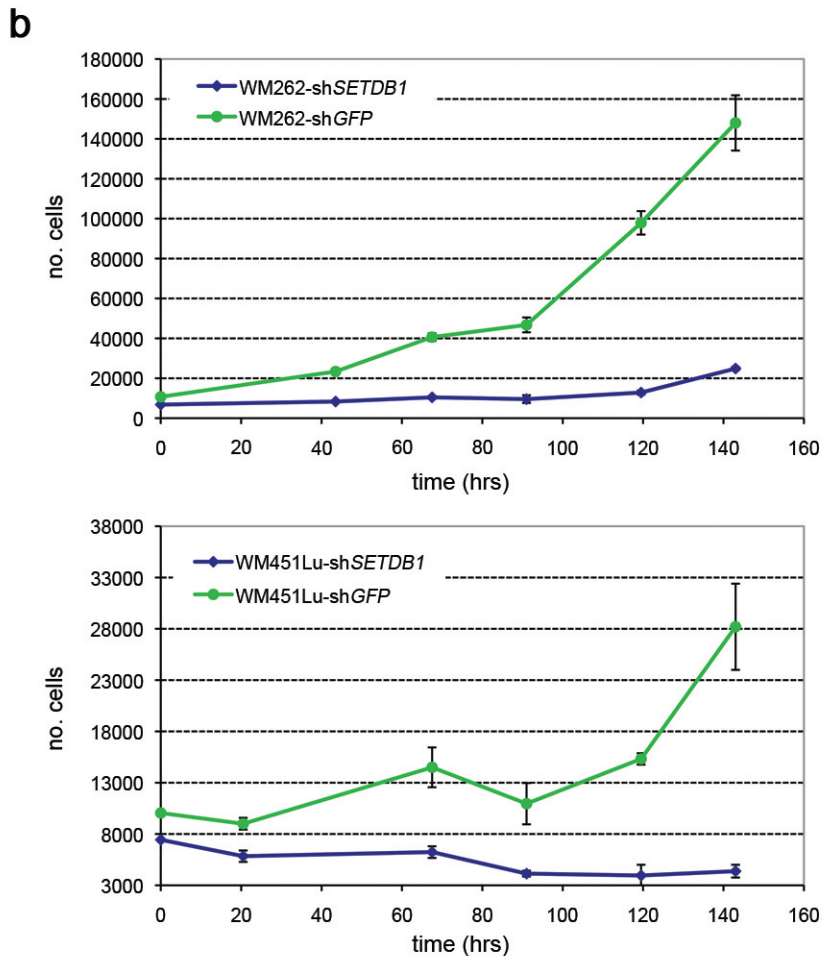
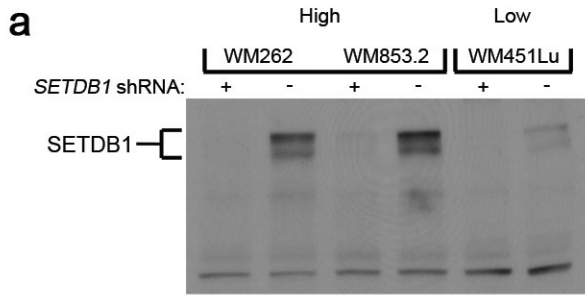
600
 GCT ACA GTG AAA TCT
 CGA TGT CAC TTT AGA
A T V K S



A375 *BRAF(V600E)* homozygous

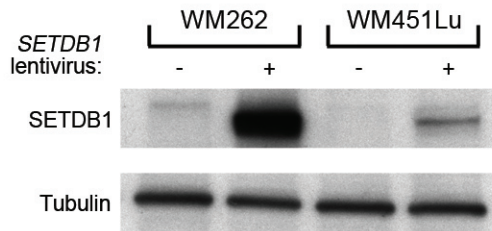
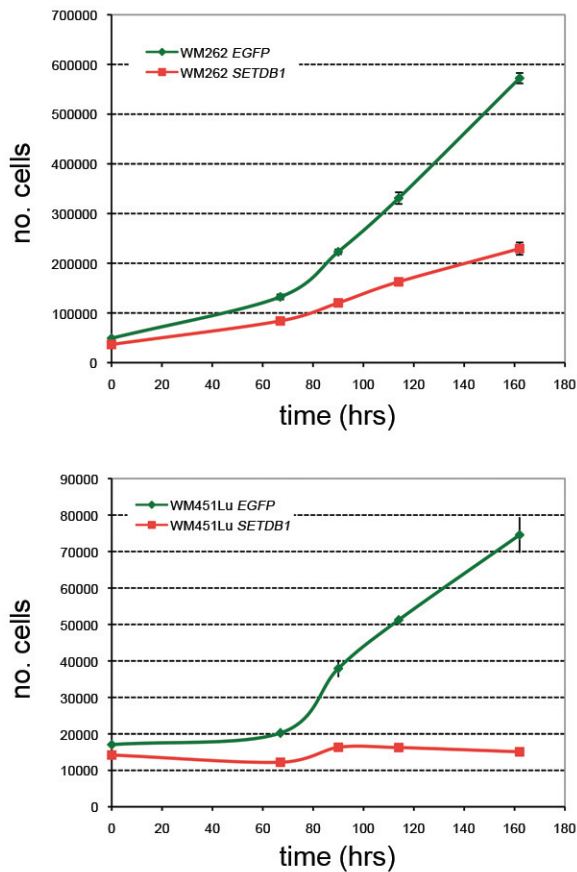
600
 GCT ACA GAG AAA TCT
 CGA TGT CTC TTT AGA
A T E K S

Supplementary Figure 9 | The WM262 SETDB1-high short-term culture is *BRAF(V600E)*-mutant
 The SETDB1-high line used for ChIP-Seq, WM262, is *BRAF(V600E)* mutant (middle). Control *BRAF* wild-type (top) and *BRAF(V600E)* mutant (bottom) cells are shown. WM451Lu was previously identified to be *BRAF(V600E)* mutant². The different areas under the nucleotide peaks likely reflect a higher *BRAF(V600E)* to *BRAF(WT)* copy number ratio in WM262 cells. The sequence reads shown were obtained from the non-coding DNA strand.

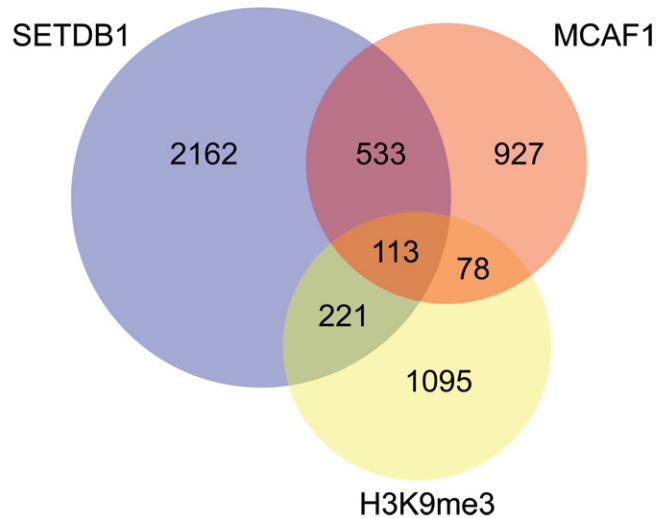


Supplementary Figure 10 | shRNA-mediated knockdown of SETDB1 is associated with reduced proliferation

a, SETDB1 protein levels are reduced in melanoma short-term cultures infected with *SETDB1* shRNA. **b**, WM262 and WM451Lu were infected with lentiviral vectors encoding *SETDB1* or *GFP* (control) shRNAs. Melanoma cultures infected with *SETDB1* shRNA showed reduced proliferation as compared to cultures infected with *GFP* shRNA. Error bars indicate the standard deviation of three replicates counted following infection.

a**b**

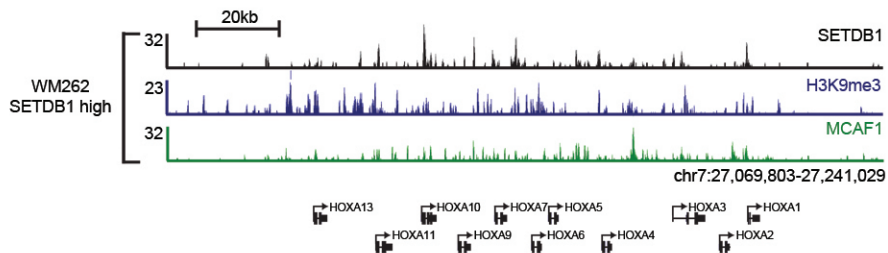
Supplementary Figure 11 | *SETDB1* overexpression affects WM262 and WM451Lu proliferation
a, *SETDB1* protein levels are elevated in melanoma short-term cultures infected with *SETDB1* lentivirus. **b**, WM262 and WM451Lu were infected with lentiviral vectors encoding *SETDB1* or *EGFP* (control). Overexpression of *SETDB1* had a detrimental effect on proliferation of both short-term cultures. The effects of *SETDB1* overexpression may differ depending on whether overexpression is achieved in cells from established tumors as compared to developing melanocytes and tumors, as in the miniCoopR assay. Error bars indicate the standard deviation of three replicates counted following infection.

a

$$\frac{\text{SETDB1 only-bound + H3K9me3 marked}}{\text{SETDB1 only-bound genes total}} = \frac{221}{(221+2162)} = 9.3\%$$

 $p=3.3 \times 10^{-9}, \chi^2$

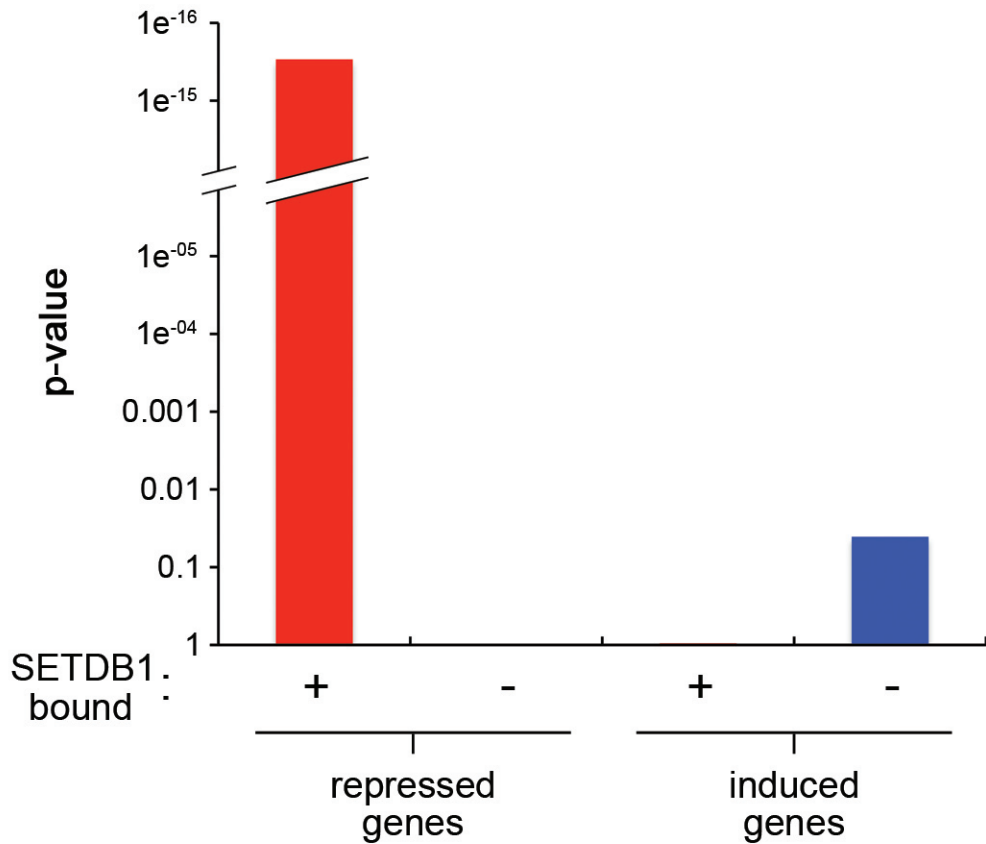
$$\frac{\text{SETDB1 and MCAF1-bound + H3K9me3 marked}}{\text{SETDB1-and MCAF1-bound genes total}} = \frac{113}{(113+533)} = 17.6\%$$

b

Supplementary Figure 12 | MCAF1 ChIP-Seq

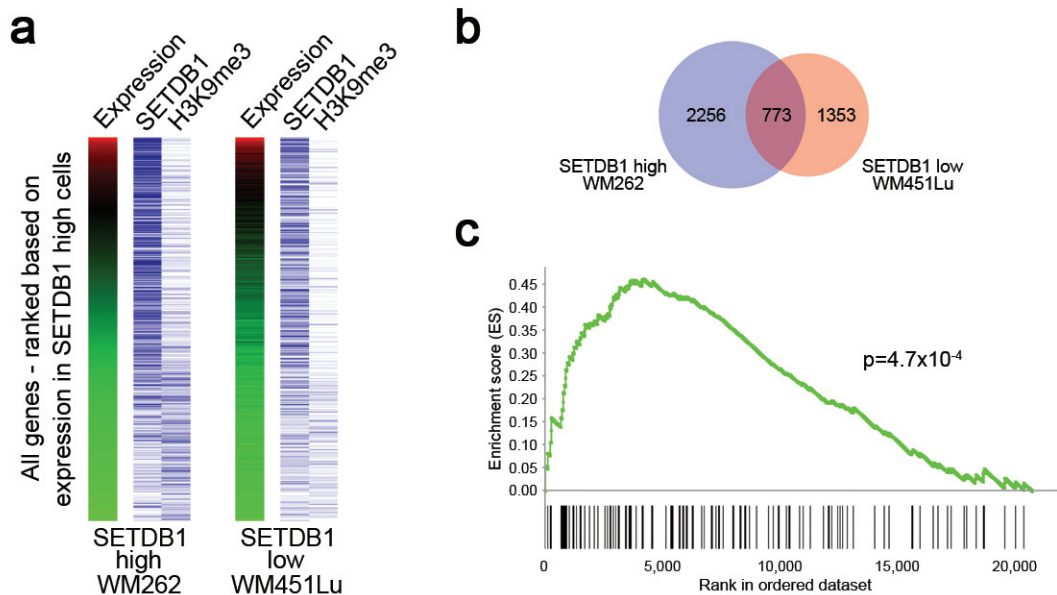
a, Significant enrichment of H3K9me3 at genes bound by both SETDB1 and MCAF1/hAM, a SETDB1 cofactor that stimulates its methyltransferase activity. (top) Venn diagram of genes bound by SETDB1, MCAF1 and marked with H3K9me3 in SETDB1-high (WM262) cells (1e-12, 1e-09 and 1e-09 cutoffs were applied, respectively). (bottom) The set of genes bound by both SETDB1 and MCAF1 is more enriched for H3K9me3 than the gene set bound only by SETDB1 ($p=3.3 \times 10^{-9}$, χ^2).

b, Included among the promoters bound by MCAF1/hAM are those of 10 of 11 HOXA genes. SETDB1, H3K9me3 and MCAF1/hAM profiles at the HOXA locus in SETDB1-high melanoma cells. The number of sequence reads is shown on the y axis.



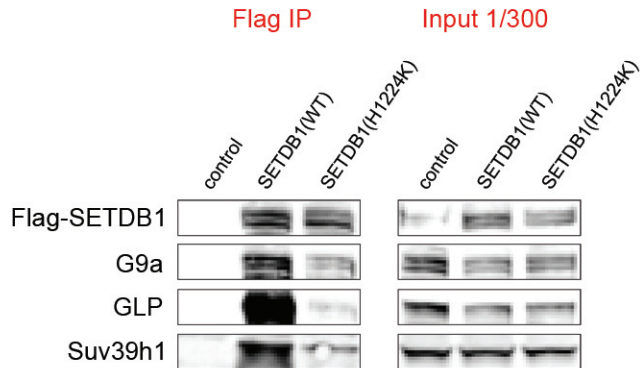
Supplementary Figure 13 | *SETDB1* overexpression causes downregulation of *SETDB1* target genes

For each gene, the expression and t-test values for all probes mapped to that gene were averaged to produce gene-level values. Genes that had an average t-test value below 0.05 were selected and split into repressed and induced classes based on the *SETDB1*/GFP ratio. Genes were annotated for the presence of a *SETDB1*-enriched region ($1e^{-12}$ cutoff) in the 10kb upstream of that gene's transcriptional start site or within the gene body. We then used a hypergeometric test to calculate a p-value for that group of genes being enriched for the binding (or absence of binding) of *SETDB1*. The averaged gene level data and binding annotation are in Supplementary Table 3.



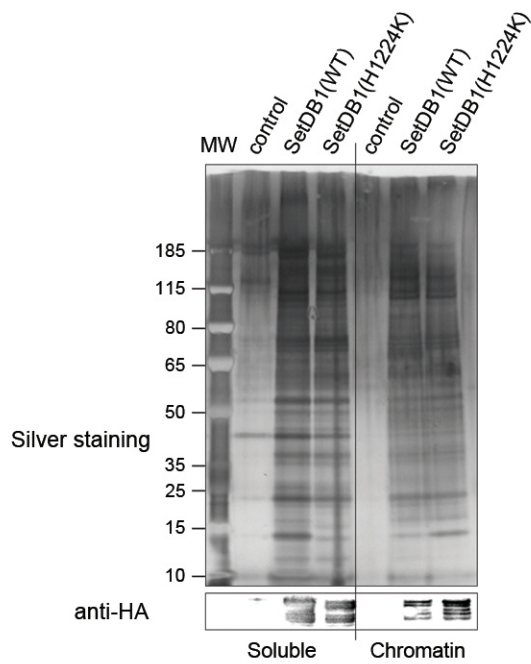
Supplementary Figure 14 | Relationship between the expression level of genes bound by SETDB1 in WM262 and WM451Lu and the expression level of SETDB1

a, Many SETDB1 targets are not marked with H3K9me3. Comparison of gene expression and the patterns of SETDB1 binding and H3K9me3 mark in SETDB1 high and low cells. Left panels, SETDB1 bound genes are rank ordered based on expression as measured from microarray experiments, with each gene normalized to the median level of expression. Right panels, genes occupied by SETDB1 and H3K9me3 are shown as blue lines. SETDB1-bound and H3K9me3-marked genes are listed in Supplementary Table 1. **b**, Defining genes bound by SETDB1 in both WM262 and WM451Lu cells. Venn diagram of genes bound by SETDB1 in SETDB1 high and low cells (Supplementary Table 1; $1e10^{-12}$ cutoff) indicates a set of genes bound in both melanomas. **c**, This "bound-bound" gene set is positively correlated by GSEA with SETDB1 expression status, suggesting an increase in SETDB1 is associated with increased expression of a subset of SETDB1 target genes. Graphical representation of the rank-ordered gene list derived from a panel of human melanoma short-term cultures stratified based on SETDB1 expression level. GSEA of SETDB1-regulated genes using the set of genes bound by SETDB1 in both high and low cells. SETDB1-bound genes generally show higher expression as levels of SETDB1 increase (ES = 0.47, NES = 1.72, FDR q-val < 1×10^{-3} , $p=4.7 \times 10^{-4}$). For this analysis we used a stricter cutoff, regions with > 15 sequence reads, to obtain a "bound-bound" set of 197 genes, a set size more suitable for GSEA (<http://www.broadinstitute.org/gsea/doc/GSEAUserGuideFrame.html>). Less strict cutoffs also gave significant GSEA scores (data not shown).



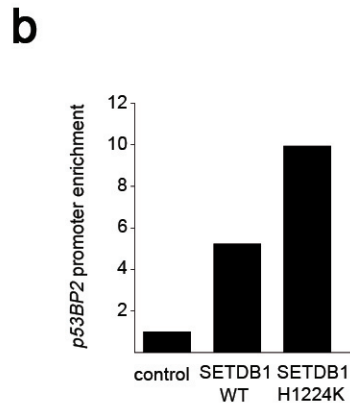
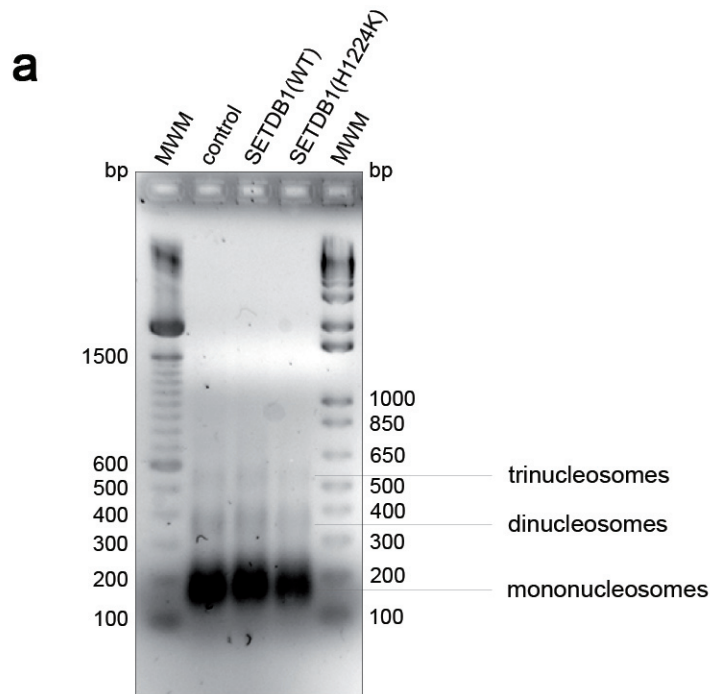
Supplementary Figure 15 | Enzymatic-deficient SETDB1 coimmunoprecipitates with other HMTase complex proteins

Anti-Flag immunoprecipitation using nuclear extracts from control C2C12 cells (lane 1), and C2C12 cells expressing Flag-HA-SETDB1(WT) (lane 2) or Flag-SETDB1(H1224K) (lane 3). Precipitated material was analyzed by western blotting using the antibodies shown on the left. Since Flag-SETDB1, G9a and GLP migrate closely (top half of the membrane), we revealed them on the same membrane piece that had been stripped between two western blot analyses. Exposure times for the immunoprecipitated products and inputs are not the same.



Supplementary Figure 16 | Levels of immunoprecipitated proteins used in histone methylation assays

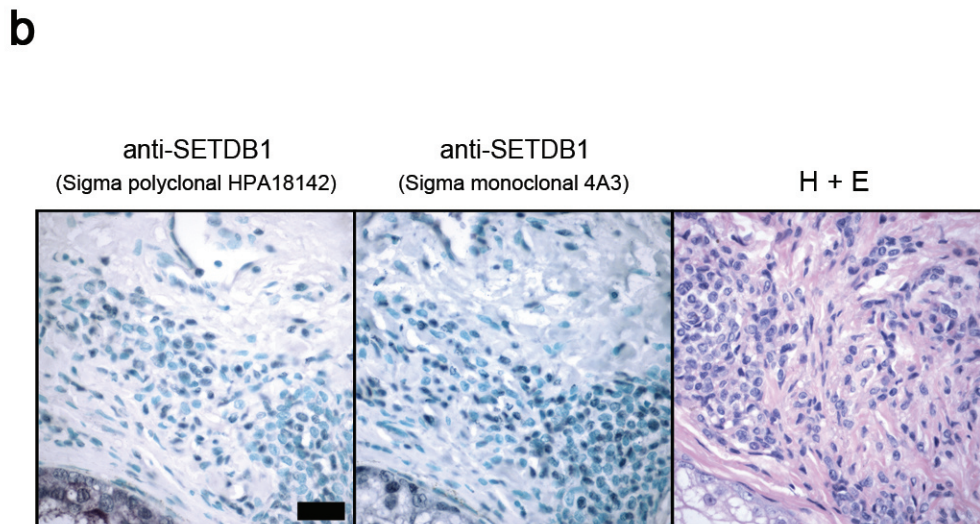
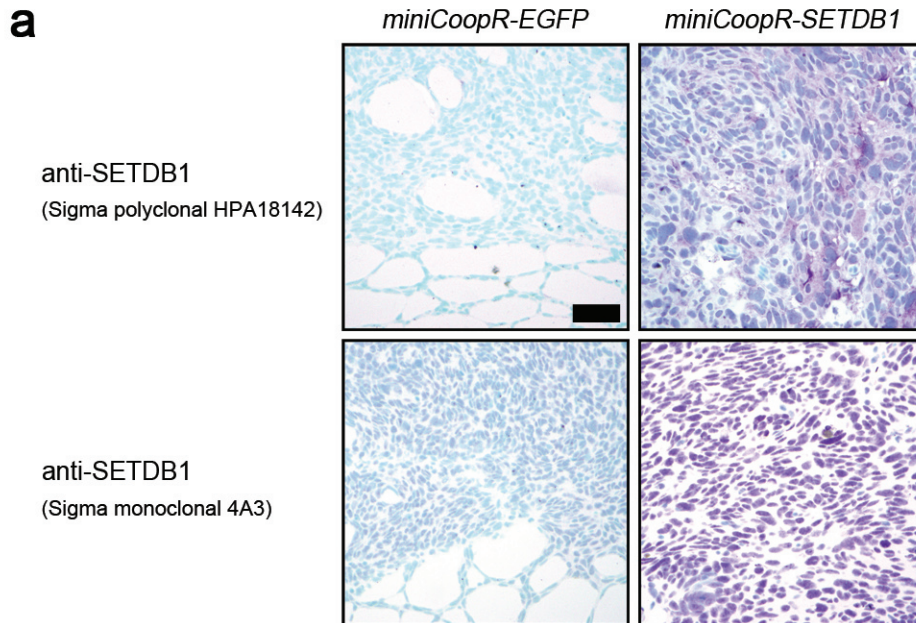
Silver staining of complexes purified for methylation assays. SETDB1(WT) and SETDB1(H1224K) were revealed using anti-HA.



Supplementary Figure 17 | Enzymatic-deficient SETDB1 binds to the SETDB1-target gene *p53BP2*

a, Agarose gel analysis and ethidium bromide staining of DNA recovered from SETDB1 immunoprecipitates. Results indicate enrichment of mononucleosomes.

b, qPCR of the *p53BP2* gene in the immunoprecipitates.



Supplementary Figure 18 | SETDB1 antibody specificity

a, Immunohistochemistry performed on zebrafish melanomas from *miniCoopR-EGFP* or *miniCoopR-SETDB1* animals. Two independent antibodies were identified that recognize human SETDB1 protein in *miniCoopR-SETDB1* melanomas. Only the methyl green counterstain is evident in anti-SETDB1 stained *miniCoopR-EGFP* melanomas. Scale bar = 70µm. **b**, Immunohistochemistry performed on human nevi demonstrate similar staining using two independent anti-SETDB1 antibodies (left, middle). H+E staining is shown (right).

1. Lister, J.A., Robertson, C.P., Lepage, T., Johnson, S.L., & Raible, D.W., nacre encodes a zebrafish microphthalmia-related protein that regulates neural-crest-derived pigment cell fate. *Development* **126** (17), 3757-3767 (1999).
2. Lin, W.M. et al., Modeling genomic diversity and tumor dependency in malignant melanoma. *Cancer Res* **68** (3), 664-673 (2008).